Applied Radiation and Isotopes 191 (2023) 110528

Contents lists available at ScienceDirect

Applied Radiation and Isotopes

journal homepage: www.elsevier.com/locate/apradiso

Unmanned stationary online monitoring system based on buoy for marine gamma radioactivity

Jinlin Song [a], Pin Gong [a,b,*], Peng Wang [c], Jinzhao Zhang [d], Zhimeng Hu [a,b], Cheng Zhou [e], Xiaoxiang Zhu [e], Qing Wei [f], Jian Zhou [f], Xiaobin Tang [a,b]

[a] Department of Nuclear Science and Technology, Nanjing University of Aeronautics and Astronautics, Nanjing, 211106, China
[b] Key Laboratory of Nuclear Technology Application and Radiation Protection in Astronautics, Ministry of Industry and Information Technology, Nanjing University of Aeronautics and Astronautics, Nanjing, 211106, China
[c] School of Environmental and Biological Engineering, Nanjing University of Science and Technology, Nanjing, 210094, China
[d] Third Institute Oceanography Ministry of Natural Resources, Xiamen, 361005, China
[e] Jiangsu Nuclear and Radiation Safety Supervision and Management Center, Nanjing, 210019, China
[f] Jiangsu Province Nuclear Radiation Science and Technology Co., Ltd, Nanjing, 210019, China

ARTICLE INFO

Keywords:
Marine gamma radioactivity monitoring
Unmanned online monitoring system
Detection efficiency calibration
Data collection and transmission

ABSTRACT

Research on unmanned online monitoring equipment for marine radioactivity surrounding nuclear power plants is of great significance. In this work, a small radioactivity monitoring system based on buoy was designed and manufactured for the emergency situation of nuclear accidents. The core of the radioactivity monitoring system is the underwater gamma spectrometer. The spectrometer can respond to gamma rays from 60 keV to 3 MeV, and can identify the nuclides whose characteristic rays belong to this energy range. The detection efficiency curve was calculated through Monte Carlo simulation and verified in a standard liquid source. A data acquisition processor was also designed to coordinate the detectors in the system and wirelessly transmit online monitoring data. Three experiments were carried out in the seawater around the Tianwan Nuclear Power Plant in Lianyungang, China using this online marine radioactivity monitoring system based on buoys. The stability and radioactivity monitoring capabilities of the system have been verified.

1. Introduction

Most nuclear power plants are built in coastal areas, making the monitoring of the marine radioactive environment critical, especially when an accident of radioactive material leakage occurs. The traditional methods of marine radioactive environmental analysis in laboratories are based on in-situ marine sampling and have high sensitivity (Bokor et al., 2016; Gaur, 1996; Povinec et al., 2001; Su et al., 2000). These methods are unsuitable for emergency monitoring of nuclear accidents with complex and changeable radiation fields due to the lack of real time and autonomy. Since the 1950s, researchers have been exploring and developing various online monitoring methods and equipment for marine radioactivity (Byun et al., 2020; Jones, 2001; Lee et al., 2019; Osvath et al., 2005; Tsabaris et al., 2008, 2021). Particularly in the past few decades, a number of marine radioactivity monitoring devices based on gamma spectrometers and seawater gamma spectroscopy methods have emerged. Admittedly, the minimum detectable activity (MDA) concentration of the sampling-free online monitoring method based on gamma spectrometers is inferior to that of the laboratory analysis method. However, real-time online monitoring can rapidly and continuously provide feedback on radioactivity data in seawater and provide early warning at critical moments (Alexakis and Tsabaris, 2021). The timely provision of sufficient radioactivity monitoring data is of great significance in nuclear accident emergency response.

Existing marine environment monitoring systems, especially those that contain the radioactivity measurement functions, use large buoys as carriers because of low system integration (Aakenes, 1995; Byun et al., 2020; Lee et al., 2019; Osvath et al., 2005; Soukissian & Chronis, 2000; Tsabaris et al., 2008, 2021; Wedekind et al., 1999). However, the transportation of large buoys requires trucks and large-scale boats, and the crane must be equipped for deployment. There is no doubt that it will increase operating costs and waste time and resources. When a nuclear accident occurs, the bulkiness of large buoys makes it difficult to realize the rapid and multi-point deployment. According to the requirements of

* Corresponding author. Jiangjun Avenue 29, Jiangning District, Nanjing, 211106, PR China.
E-mail address: gongpin@nuaa.edu.cn (P. Gong).

https://doi.org/10.1016/j.apradiso.2022.110528
Received 9 June 2022; Received in revised form 20 October 2022; Accepted 21 October 2022
Available online 1 November 2022

nuclear accident emergency, an online marine radioactivity monitoring system based on small buoys has been developed in this work. Meanwhile, the measurement accuracy and operational stability of the system were measured through three deployment tests. The online marine radioactivity monitoring system with flexibility, radioactivity monitoring automation and radioactivity measurement accuracy has higher practicability and better economy.

2. Hardware design of the system

2.1. Overall structure of the system

The developed online marine radioactivity monitoring system consists of a moored buoy body, a dose rate meter (GM-Tubes 712, LND, USA), a data acquisition processor, an underwater gamma spectrometer (GM-Tubes ZP1314, Centronic, UK and NaI(Tl) detector, BRIDGEPORT Instruments, LLC, USA), a meteorological sensor (Weather Station 150WX, AIRMAR, USA), a navigation light, a solar panel, and a Li-ion battery (12 V, 40 Ah). Fig. 1 is the structural diagram of this system. The selected mooring buoy weighs 70 kg. Hence, it can be transported on the ocean by a small boat and deployed by only a few adults. The self-designed gamma spectrometer is installed at the bottom of the buoy to measure the dose rate and the activity concentration of radionuclides in seawater. The dose rate meter, a set of double GM tubes, is used to measure the air dose rate on the sea. The design of this dose rate meter based on double GM tubes is referred to in the earlier study of our team (P. Wang et al., 2018). The meteorological sensor can monitor the maritime meteorological data, such as temperature, humidity, and wind velocity. The data acquisition processor can receive the data detected by the underwater gamma spectrometer, the dose rate meter and the meteorological sensor, and upload the data to the Elastic Compute Service (ECS). Accordingly, the terminal software can wirelessly receive the measurement results from the sea. The data acquisition processor can also receive control commands from the terminal software to modify the working parameters of the detectors. The main performance parameters of the system are shown in Table 1.

In the event of a nuclear accident, lightweight and miniature radiation monitoring buoy systems can be deployed at multiple points to form a marine radiation monitoring network. The terminal software has been designed with the function to allow simultaneous reception of multiple data packets from various monitoring buoys. Fig. 2 shows the general working mode of the radiation monitoring network. Multiple online marine radioactivity monitoring systems are deployed in the offshore area covered by fourth-generation (4G) signal upload monitoring data to the cloud server in real time. Then, the terminal software can receive

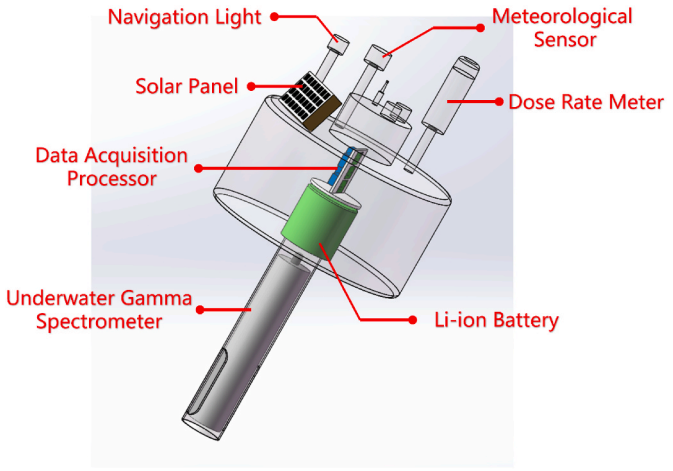

Fig. 1. Structural diagram of the marine radioactivity online monitoring system.

Table 1
Performance parameters of the marine radioactivity online monitoring system.

Parameter Name	Parameter Value
Size of the system	Φ 0.7m × 1.5m
Weight of the system	≤70 kg
Operating depth in ocean	≤500 m
Duration of the system	10–17 days
Power consumption of the underwater gamma spectrometer	1.8 W
Communication methods	4G network communication technology
Energy response range	60 keV–3 MeV
Energy resolution	6.7% (^{137}Cs)
Identifiable nuclides	^{40}K, ^{137}Cs, ^{60}Co, ^{134}Cs, ^{131}I, ^{208}Tl, ^{214}Bi, ^{214}Pb, ^{226}Ra, and ^{232}Th
MDA	0.27 Bq/L (^{137}Cs, 30 min)
Detection range of the underwater dose rate	NaI(Tl) detector: 1−10^5 nGy/hGM counter tube: 10^4–10^9 nGy/h
Detection range of the air dose rate	10–10^6 nGy/h

monitoring data at any place with the internet. The feasibility of radiation online monitoring networks based on the mobile communication technology will be greater with the improvement of maritime mobile signal base stations (BS).

2.2. Data acquisition processor

The data acquisition processor is the core of the entire system, and its composition relationship is shown in Fig. 3 The data acquisition processor can realize the acquisition, processing, storage, and transmission of data through its circuit composition: master control circuit, clock circuit, data communication circuit, watchdog circuit, and power management circuit. The master control circuit uses the RS232 standard and SPI communication protocol to collect detection data from the underwater gamma spectrometer, dose rate meter, and meteorological sensor. The above-mentioned data is packaged by the microcontroller (AM335X) of the master control circuit and stored on the secure digital memory card (SD card) of the data communication circuit module through SPI. Benefiting from the extensive coverage of the 4G wireless network, the data communication circuit uses the data transfer unit (F2910) to achieve remote wireless transmission of data streams and telecontrol of the system. Under the 4G network, the packaged data is uploaded to the cloud server. Then, the terminal downloads the data package through the network and visualizes the data. This data communication method not only has low power consumption and large data traffic but also avoids data loss caused by accidental shutdown of the local server.

2.3. Underwater online monitoring gamma spectrometer

A gamma spectrometer was designed to be aimed at the measurement in seawater for a long time. The gamma spectrometer is placed in a corrosion-resistant and pressure-resistant waterproof cabin made of titanium alloy. As shown in Fig. 4, the gamma spectrometer in the waterproof cabin is composed of a NaI(Tl) detector (BRIDGEPORT Instruments, LLC), a GM counter tube (ZP1314, Centronic, UK), an energy spectral analysis module, an aluminum alloy bracket, and several PVC plastic brackets. The dimension of the NaI(Tl) crystal is Φ7.62 cm × 7.62 cm, the dimension of the NaI(Tl) detector is Φ8.72 cm × 8.97 cm, and the dimension of the gamma spectrometer is Φ10.0 cm × 63.2 cm. In the low-dose radiation field, the underwater dose rate is calculated by the G(E) function (Terada et al., 1980; Yudong et al., 2018) according to the energy spectrum measured from the NaI(Tl) detector. The GM tube placed inside the spectrometer is used to deal with underwater dose rate measurement in high-dose field, which can increase the measurement range of the underwater dose rate to 1–10^9 nGy/h. To be clear, the GM tube described here is independent of the dose rate meter described in section 2.1. However, the calibration method of the GM tubes operating

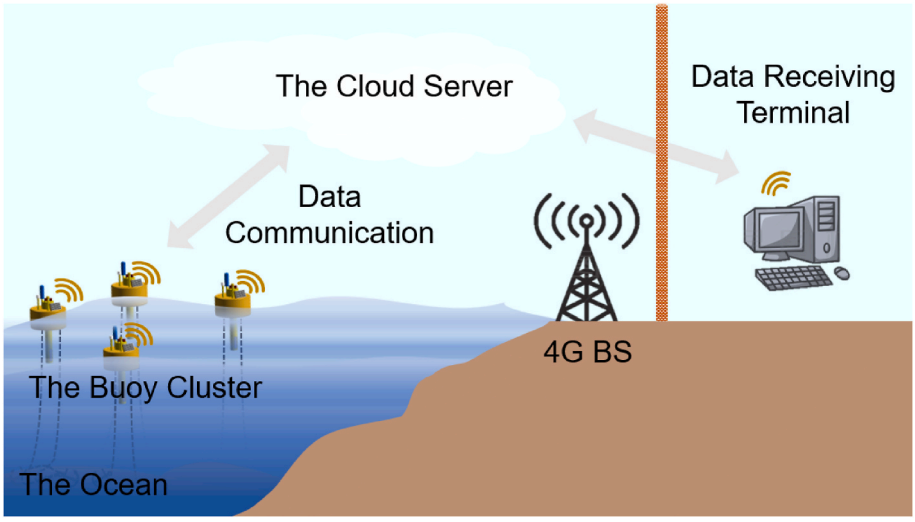

Fig. 2. Conceptual diagram of the working mode of the marine radioactivity monitoring network.

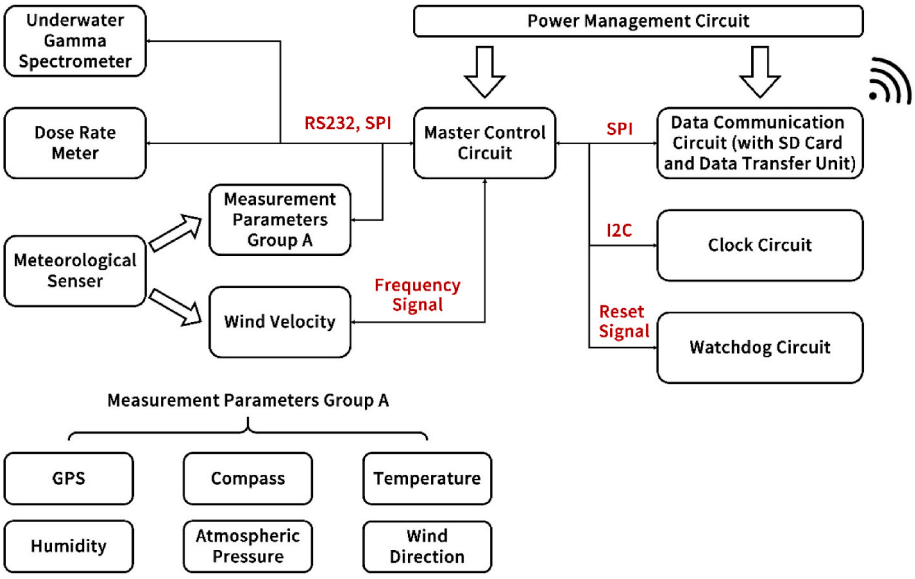

Fig. 3. Composition relationship of the data acquisition processor.

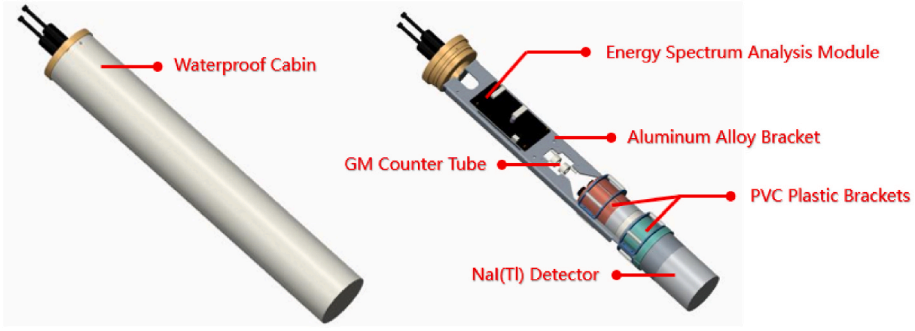

Fig. 4. Structural diagram of the underwater online monitoring gamma spectrometer.

in two different parts of the system is similar (P. Wang et al., 2018) (see Fig. 5).

The acquisition of dose rate and radionuclide information in seawater depends on the energy spectral analysis module running the algorithm of spectral analysis (Tsabaris and Prospathopoulos, 2011). The realization of the spectral analysis module involves electronic design and embedded program development. Its circuit composition can be divided into CPU, power supply and management circuit, data

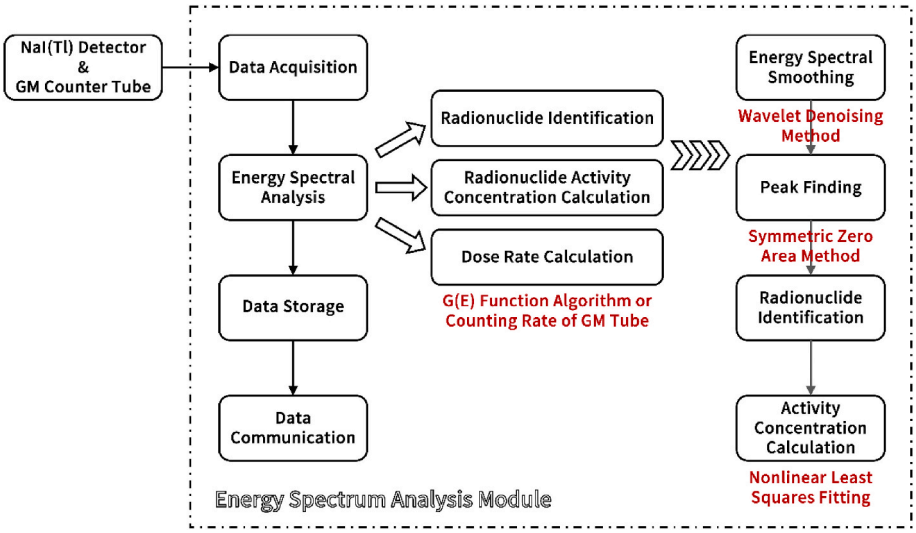

Fig. 5. Functional composition diagram of the energy spectral analysis module.

acquisition circuit, data storage circuit, ethernet communication module, real-time clock circuit, watchdog circuit, EEPROM storage circuit, and data transmission circuit. The CPU is an ARM chip of the AM335X series with Cortex-A8 high-performance processor produced by Texas Instruments. The Linux operating system (OS) was developed to realize the setting of the spectral acquisition time, spectral acquisition, spectral analysis, storage, and transmission of the spectral analysis results (Fig. 6). The peak searching algorithm has been written in this module (Liang et al., 2019; P. Wang et al., 2018; Ye et al., 2021).

3. Detection efficiency of the underwater gamma spectrometer

3.1. MCNP model of the underwater gamma spectrometer

The underwater gamma spectrometer must be calibrated to know the activity concentration of a certain radionuclide according to the spectral data. The total detection efficiency of the underwater gamma spectrometer was calculated on the basis of MCNP5-1.14 (Androulakaki et al., 2015; Brown et al., 2002; Forster et al., 2004; Y. Wang et al., 2015; Zhang et al., 2020). The geometric model of the spectrometer is shown in Fig. 7. There is a spherical cell with a radius of 100 cm outside the gamma spectrometer, and its material composition approximates the seawater environment. As a key nuclide to assess the level of radioactive contamination, the saturated penetration distance of ^{137}Cs in seawater (seawater thickness with 0.1% net particle transmittance) determines the lower limit of the size of seawater cell. It's averagely 1 m underwater where the sensitive volume of the detector works, when the small size buoy is floating at sea. And the net transmittance of 2.614 MeV photons is 1.28% when the seawater thickness is 100 cm, which is considered to be an effective shielding of radioactivity in the air. The relationship between the seawater thickness and the particle transmittance is shown in Fig. 8. Because of the above three reasons, the seawater environment cell was determined to be a sphere with a radius of 100 cm. The geometric center of NaI(Tl) crystal coincides with the spherical center of seawater environment cell. And the source term was the single-energy photons uniformly distributed in the seawater environment cell. 54 values taken at intervals of 0.05 MeV from 0.05 MeV to 2.7 MeV was used as the energy value of the source term. The simulation result of detection efficiency was fitted by Formula (1) (Ahmadi et al., 2018; Knoll, 2010). The fitted curve is shown in Fig. 9, and R^2, the goodness of fit, reaches 0.9775.

$$\ln \varepsilon_\gamma = \sum_j P_j (\ln E_\gamma)^j, \tag{1}$$

where $j = 0$–6, E_γ is the energy of the gamma rays, ε_γ is the detection efficiency when the energy of gamma rays is E_γ, and P_j is the parameter to be calculated.

The error of the simulation of detection efficiency is less than 0.052, if the extreme case when the energy is 0.05 MeV is not considered. The simulation error of the γ-ray energy of 0.05 MeV is obviously higher, which should be because this energy value is lower than the energy response lower limit of the underwater gamma spectrometer designed in

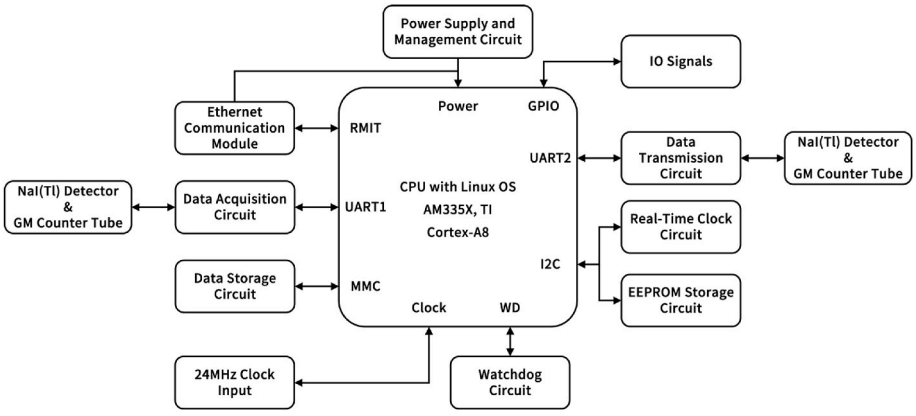

Fig. 6. Circuit composition diagram of the energy spectral analysis module.

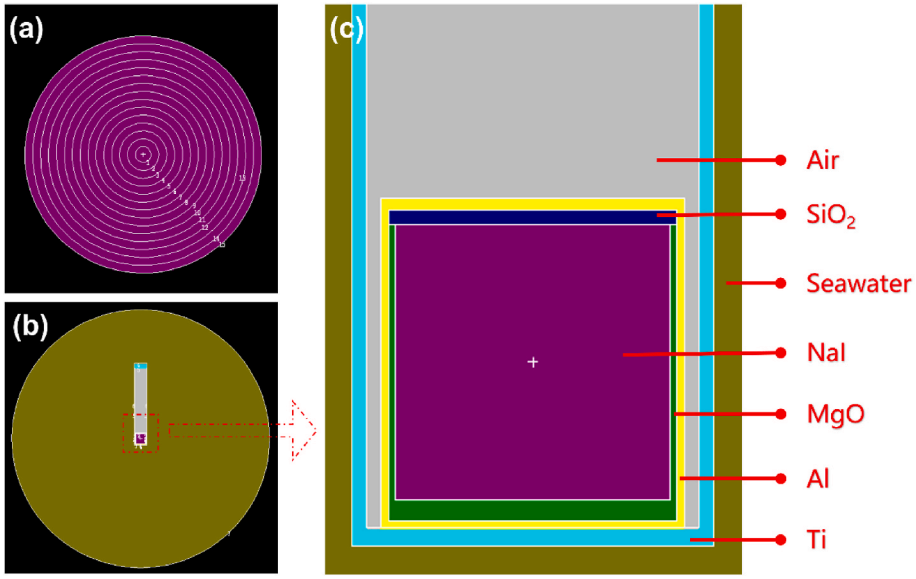

Fig. 7. (a) Is the MCNP model to simulate the transmittance of gamma rays in the seawater. (b) and (c) are the MCNP models of the underwater gamma spectrometer.

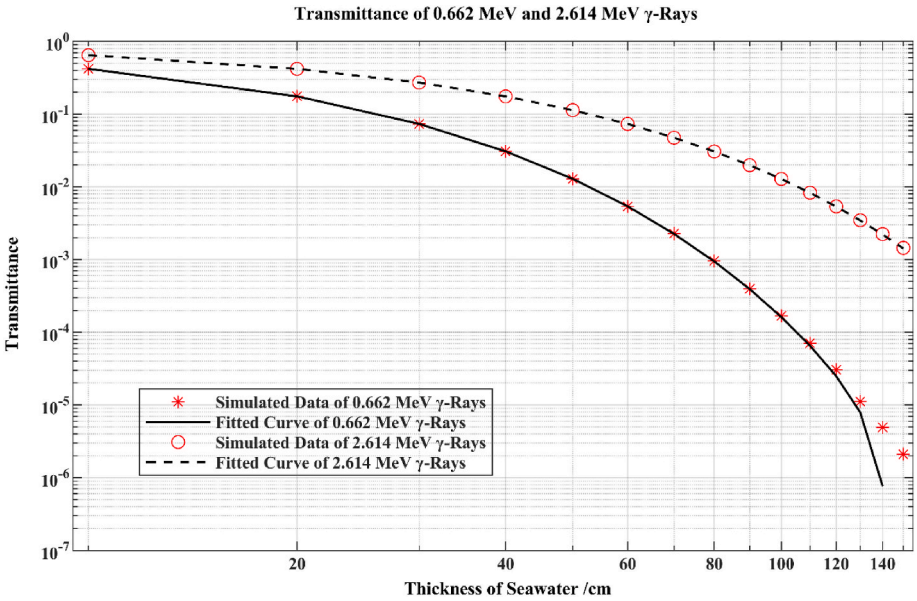

Fig. 8. Fitted curve of the relationship between the gamma rays transmittance and seawater thickness.

this report.

3.2. Experimental verification of the efficiency calibration curve

The detection efficiency calibration curve calculated in the previous section was verified in the standard liquid source provided by the National Ocean Technology Center, China. This liquid source has a diameter of 2 m and a height of 2 m and contains radionuclides ^{133}Ba (1 Bq/L), ^{137}Cs (1 Bq/L), and ^{40}K (12 Bq/L). The underwater gamma spectrometer measured 15 times for 1 h in the liquid source. The activity concentration of the three radionuclides was calculated using the detection efficiency calibration curve. The average activity concentrations of the three nuclides measured by the underwater gamma spectrometer in the standard liquid source are 0.960 Bq/L, 0.957 Bq/L, and 13.643 Bq/L, with standard deviations of 0.119 Bq/L, 0.094 Bq/L, and 0.960 Bq/L. The average dose rate in the liquid source is 3.58×10^{-3} μGy/h with the standard deviation of 2.68×10^{-5} μGy/h. The measurement values of ^{133}Ba and ^{137}Cs have relative errors less than 5% compared with the reference values. The measurement of ^{40}K has a relative error of 13.7% due to the influence of the natural background radiation environment. This value is within the acceptable error range. Finally, the detection efficiency calibration curve calculated in Section 3.1 was adopted.

3.3. MDA calculation of the underwater gamma spectrometer

MDA is a significant parameter to measure detector sensitivity. Specifically, the MDA in this work refers to the minimum detectable activity concentration because the detection efficiency is a quantity related to the volume of seawater. The accepted calculation formula of MDA is shown as Formula (2) (Bagatelas et al., 2010; Han et al., 2020; Zhang et al., 2020).

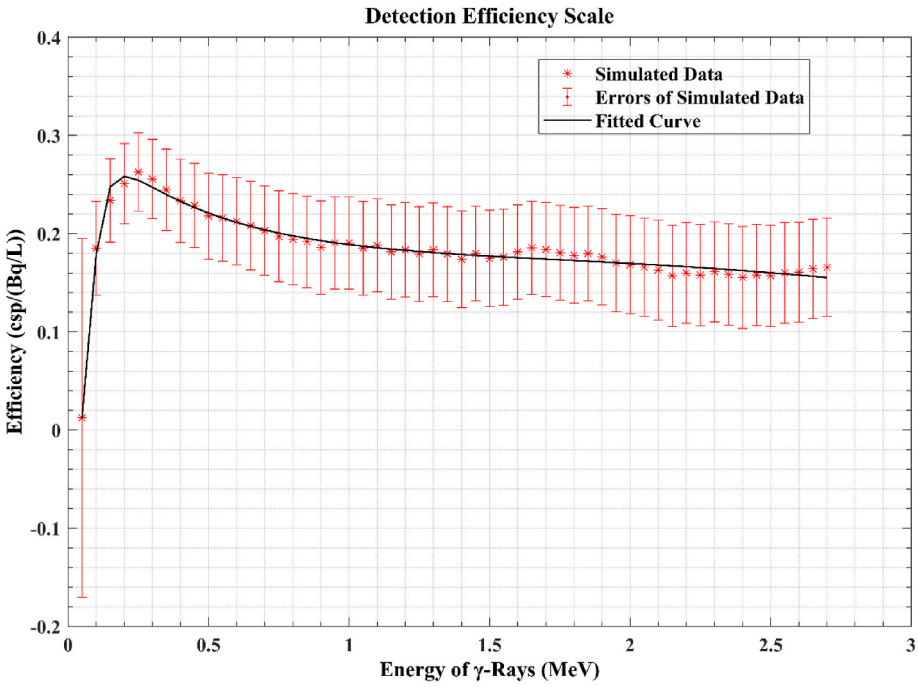

Fig. 9. Fitted curve of the relationship between the detection efficiency and the energy of gamma rays, and the error of the simulation of detection efficiency.

$$MDA = \frac{L_D}{\varepsilon_\gamma * I_\gamma * T} = \frac{2.17 + 4.65B^{1/2}}{\varepsilon_\gamma * I_\gamma * T}, \quad (2)$$

where L_D is the detection limit; B is the sub-peak count of the background spectrum, which is measured by the underwater gamma spectrometer in the real seawater environment; ε_γ is the detection efficiency, which is calculated by the fitting curve in Section 3.1; I_γ is the emission probability of the gamma rays; and T is the spectral acquisition time. According to the measured spectrum of the underwater gamma spectrometer in seawater, the MDA of the radionuclides was obtained, as shown in Table 2.

4. Deployment tests of the system in marine environment

The marine radioactivity online monitoring system has carried out three field deployment tests in the seawater around Tianwan Nuclear Power Station in China. The working performance of the air dose rate meter, underwater gamma spectrometer, meteorological sensor, data acquisition processor, and buoy in the marine environment was experimentally verified. Three implementations of the deployment tests were aimed to optimize the design of the system according to the natural environment, and to determine the appropriate operating method to guide future practical applications (Fig. 10).

Table 2
MDA of radionuclides under different spectral acquisition time.

Acquisition Time (s)	^{40}K (Bq/L)	^{137}Cs (Bq/L)	^{60}Co (Bq/L)	^{134}Cs (Bq/L)	^{131}I (Bq/L)	^{208}Tl (Bq/L)	^{214}Bi (Bq/L)
60	9.65	1.71	1.21	1.49	1.73	0.56	3.76
300	3.72	0.70	0.48	0.61	0.72	0.17	1.23
1800	1.40	0.27	0.18	0.24	0.28	0.05	0.41
3600	0.97	0.19	0.13	0.17	0.20	0.04	0.28
14,400	0.48	0.06	0.06	0.08	0.10	0.02	0.13
43,200	0.27	0.03	0.03	0.05	0.06	0.01	0.07

4.1. First deployment test

The first deployment site was selected within 1 km from the discharge outlet of Tianwan Nuclear Power Station to verify the detection ability of the system for artificial radionuclides. The water depth of the deployment site was 2.5 m at the time of deployment, and the depth was 1 m at the lowest tide level. The detection sensitive device of the gamma spectrometer was located at 1 m underwater, and the detector could touch the seabed at the lowest tidal level. This test started at 12:17 on November 12, 2020 and ended at 21:28 on November 22, 2020. As shown in Fig. 11, the dose rate of the seawater is consistent with the activity concentration of ^{40}K. During the first test, the dose rate of the seawater varies from 1 nGy/h to 66.5 nGy/h. However, the normal range of the seawater dose rate at that point was 1 nGy/h to 3 nGy/h. In Fig. 12, the tidal variation diagram of seawater, the dose rate begins to exceed 3 nGy/h when the tidal height is lower than 2 m, and the dose rate reaches the peaks when the tidal height is lower than 1 m. For example, when the tide is at the lowest level on November 16, the peaks of dose rate and the activity concentration of ^{40}K occur during the same period. Therefore, the dose rate above 3 nGy/h may be the contribution of seabed sediments. Most of the measured data were not received from November 13 to November 15, 2020 and from November 20 to November 22, 2020, due to the accidental closure of the local data receiving server. In addition, there are many cases where ^{40}K cannot be identified because the spectral acquisition time was 1 min.

Some problems were revealed in the first deployment test: (a) there were frequent failures in the wireless data transmission; (b) the radionuclides could not be identified because the spectrum acquisition time was set too short; (c) and the measurement values were extremely inaccurate because the water level at the selected deployment site was always so low that the underwater gamma spectrometer touched the seabed and the buoy was tilted greatly.

4.2. Second deployment test

Before the second experiment, the software was optimized to solve the data loss during the data reception, and the spectral acquisition time was increased to 30 min to reduce the MDA of the underwater gamma

Fig. 10. The marine radioactivity online monitoring system working in the seawater.

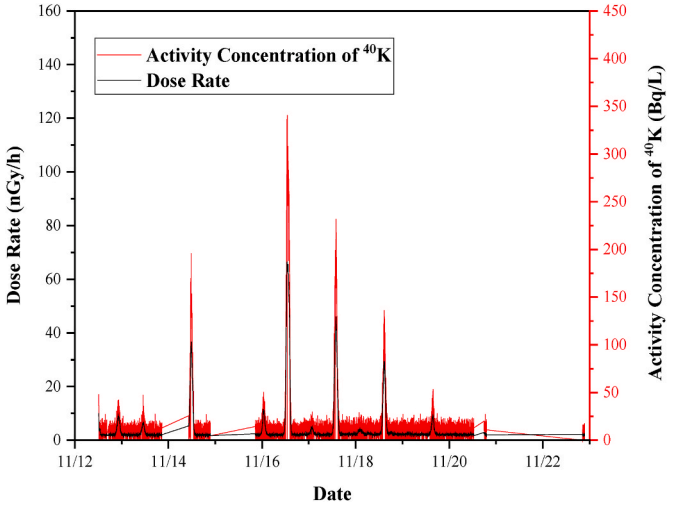

Fig. 11. Measurement results of the activity concentration of ^{40}K and the seawater dose rate during the first deployment.

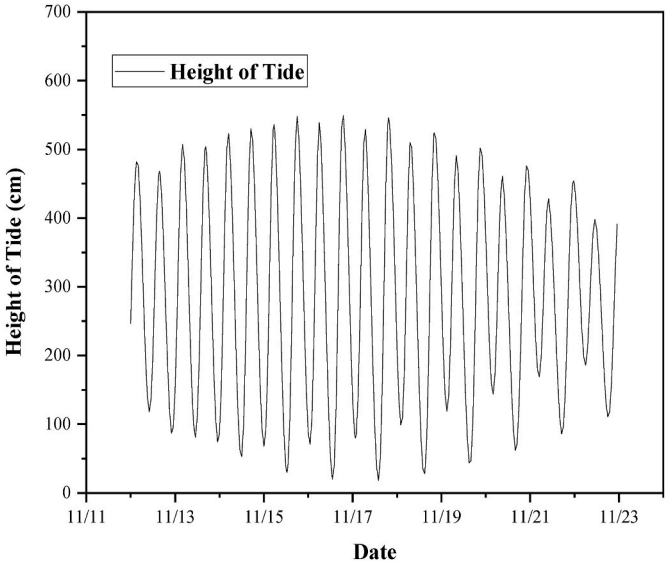

Fig. 12. Tidal variation during the first deployment.

spectrometer. This site is the marine monitoring point position of off-site emergency of Tianwan Nuclear Power Station. The deployment experiment at this location is conducive to the accumulation of local background data that could provide basic data for the nuclear emergency measurement. The water depth of the deployment site was 3.5 m at the time of deployment, and the depth was 1 m at the lowest tide level for these days. This test started at 10:30 on December 4, 2020 and ended at 12:30 on December 16, 2020.

During the second deployment test, the dose rate of seawater and the activity concentration of ^{40}K were not affected by the tide for most of the time because the seawater is deeper at this location. During the period from 12:00 on December 5 to 12:00 on December 11, 2020, the tide level was stable, and the lowest value of the tide level was 103 cm. The measurement result of the activity concentration of ^{40}K is 10.3–13.8 Bq/L, the expected measured value is 11.89 Bq/L, and the standard deviation is 1.04 Bq/L. The measurement result of dose rate in seawater is 1.9–2.4 nGy/h, the expected the measured values is 2.04 nGy/h, and the standard deviation is 0.108 nGy/h. The stability of the activity concentration and dose rate measurement demonstrates the good stability of the system. The peaks that appeared in Fig. 13 are still the effect of seabed sediments because the tidal level is considerably low at that time. The operating time of the system for the second deployment has been increased from 10 days to 14 days, even if the weather is cold in winter, because the navigation light is replaced by another one with a solar panel. (see Fig. 14)

4.3. Third deployment test

Before the third deployment, the software of the system was further optimized. First, the data receiving terminal is changed from a local

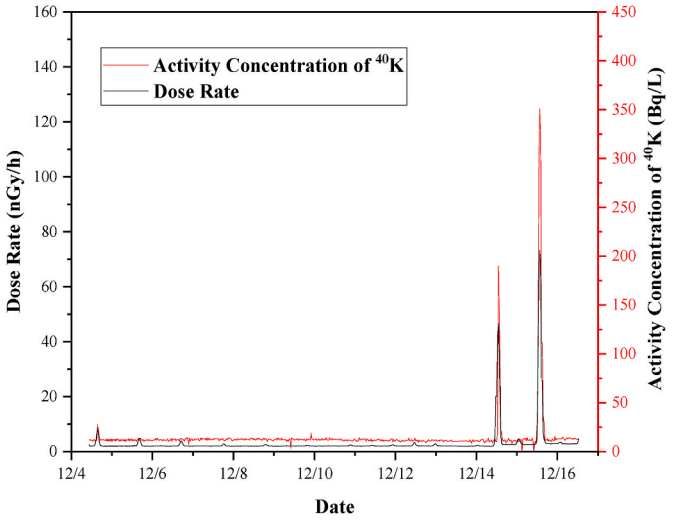

Fig. 13. Measurement results of the activity concentration of ^{40}K and the seawater dose rate during the second deployment.

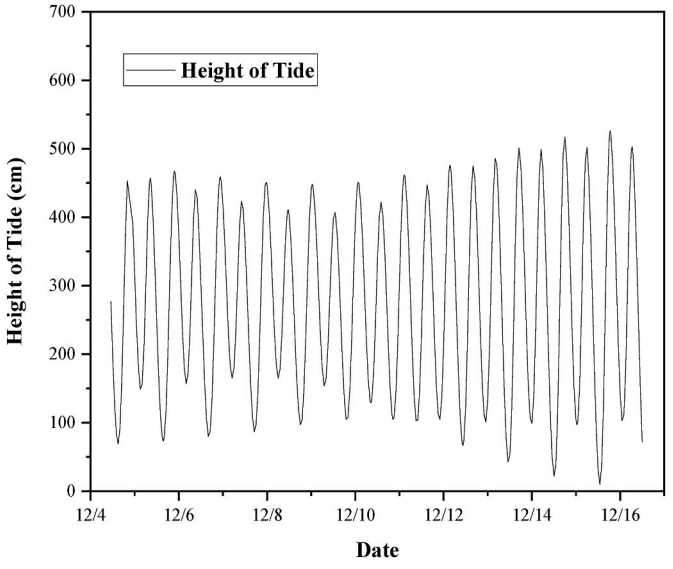

Fig. 14. Tidal variation during the second deployment.

server to a cloud server to avoid data loss due to unexpected shutdown of the server. Second, the system parameters can be remotely set through the server, such as the spectral acquisition time. The acquisition of the full-spectral data is also realized. The third deployment site is another marine monitoring point position of off-site emergency of Tianwan Nuclear Power Station. The water depth of the deployment site was 6 m at the time of deployment, and the depth was 4 m at the lowest tide level for these days. The influence of tide on the results of radiation measurement can be ignored during this test. This deployment test achieved a 17-day operation, from 16:29 on May 21, 2021 to 10:03 on June 1, 2021, including an 11-day offshore operation and a 6-day land operation. During the third deployment, the measurement result of the activity concentration of ^{40}K is among 4.17–18.05 Bq/L, the expected measured value is 11.265 Bq/L, and the standard deviation is 1.30 Bq/L. The measurement result of dose rate in seawater is 1.9–2.1 nGy/h, the expected measured value is 2.023 nGy/h, and the standard deviation is 0.06 nGy/h. In Fig. 15, there are several data mutations from May 21 to 22, 2021. The reason for such fluctuation is that the spectral acquisition time was only 5 min at that time, which caused the ^{40}K to be unrecognized four times.

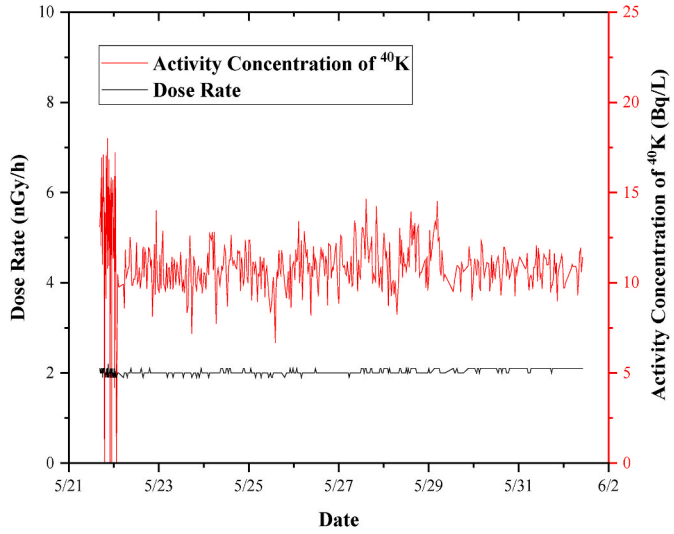

Fig. 15. Measurement results of the activity concentration of ^{40}K and the seawater dose rate during the third deployment (offshore part).

5. Conclusion

A set of online monitoring system for marine radioactive pollution based on small buoys was developed in this article, which can be applicable to nuclear emergency monitoring in the coastal areas around nuclear power plants. And the function and performance of the online monitoring system were verified through three deployment tests. The system can continuously work for 10–17 days, which meets the requirement of emergency monitoring. The test results show that the average dose rate in the sea area near Tianwan Nuclear Power Station is ~2 nGy/h, and the activity concentration of ^{40}K is ~11 Bq/L. The spectral acquisition time must be set to 30 min to ensure the accuracy of nuclide identification. The influence of seabed sediments can be prevented by choosing sites where the seawater depth is greater than 2 m at the lowest tide level. The lower limit of the seawater depth of the deployment sites is 1.2 m, otherwise the online monitoring system will be tilted and even fall down.

On the basis of miniaturization, the online marine radioactivity monitoring system realizes various functions, such as the measurement and online analysis of the underwater gamma spectrum, the monitoring of dose rate on the sea, the monitoring of marine meteorological environment, and long-distance wireless data communication. The online monitoring system has been continuously improved through the actual deployment tests, and its usage and precautions have been clarified. Each component of the system can be normally implemented, and the radioactivity level of the seawater can be accurately measured to meet the measurement requirements of accident emergency monitoring. The small and lightweight design also improves the flexibility of the marine radioactivity online monitoring system, making it a certain application prospect in the field of marine radioactivity monitoring. In the future, a redundant satellite communication function will be added to prevent network failures, and the reliability of the system will be further improved.

CRediT authorship contribution statement

Jinlin Song: Writing – review & editing, Writing – original draft, Visualization, Investigation, Formal analysis. **Pin Gong:** Writing – review & editing, Validation, Project administration, Funding acquisition, Formal analysis, Data curation, Conceptualization. **Peng Wang:** Writing – review & editing, Methodology, Funding acquisition. **Jinzhao Zhang:** Visualization, Methodology, Funding acquisition, Data curation. **Zhimeng Hu:** Writing – review & editing, Conceptualization. **Cheng Zhou:**

Supervision, Project administration, Funding acquisition. **Xiaoxiang Zhu:** Supervision, Project administration. **Qing Wei:** Validation, Project administration. **Jian Zhou:** Validation, Project administration. **Xiaobin Tang:** Writing – review & editing, Validation, Supervision, Methodology, Conceptualization.

Declaration of competing interest

The authors declare that they have no known competing financial interests or personal relationships that could have appeared to influence the work reported in this paper.

Data availability

No data was used for the research described in the article.

Acknowledgments

This work was supported by the Primary Research and Development Plan of Jiangsu Province (Grant No. BE2019727, BE2022846), the Research Project of Ecology and Environment of Jiangsu Province (Grant No. 2021012), the Fundamental Research Funds for the Central Universities (Grant No. NC2022006), and the Postgraduate Research & Practice Innovation Program of Jiangsu Province (Grant No. KYCX22_0352).

References

Aakenes, U.R., 1995. Radioactivity monitored from moored oceanographic buoys. Chem. Ecol. 10 https://doi.org/10.1080/02757549508035330, 1–2.

Ahmadi, S., Ashrafi, S., Yazdansetad, F., 2018. A method to calculate the gamma ray detection efficiency of a cylindrical NaI (Tl) crystal. J. Instrum. 13 (5) https://doi.org/10.1088/1748-0221/13/05/P05019.

Alexakis, S., Tsabaris, C., 2021. Design of an interactive cellular system for the remote operation of ocean sensors: a pilot study integrating radioactivity sensors. J. Mar. Sci. Eng. 9 (8), 910.

Androulakaki, E.G., Tsabaris, C., Eleftheriou, G., Kokkoris, M., Patiris, D.L., Vlastou, R., 2015. Seabed radioactivity based on in situ measurements and Monte Carlo simulations. Appl. Radiat. Isot. 101 https://doi.org/10.1016/j.apradiso.2015.03.013.

Bagatelas, C., Tsabaris, C., Kokkoris, M., Papadopoulos, C.T., Vlastou, R., 2010. Determination of marine gamma activity and study of the minimum detectable activity (MDA) in 4pi geometry based on Monte Carlo simulation. Environ. Monit. Assess. 165 https://doi.org/10.1007/s10661-009-0935-4, 1–4.

Bokor, I., Sdraulig, S., Jenkinson, P., Madamperuma, J., Martin, P., 2016. Development and validation of an automated unit for the extraction of radiocaesium from seawater. J. Environ. Radioact. 151 https://doi.org/10.1016/j.jenvrad.2015.08.015.

Brown, F.B., Barrett, R.F., Booth, T.E., Bull, J.S., Cox, L.J., Forster, R.A., Goorley, T.J., Mosteller, R.D., Post, S.E., Prael, R.E., Selcow, E.C., Sood, A., Sweezy, J., Brown, F. B., Goorley, J.T., 2002. Los Alamos Title: MCNP Version 5. https://mcnp.lanl.gov/pdf_files/la-ur-02-3199.pdf.

Byun, J.-I., Choi, S.-W., Song, M.-H., Chang, B.-U., Kim, Y.-J., Yun, J.-Y., 2020. A large buoy-based radioactivity monitoring system for gamma-ray emitters in surface seawater. Appl. Radiat. Isot. 162 https://doi.org/10.1016/j.apradiso.2020.109172.

Forster, R.A., Cox, L.J., Barrett, R.F., Booth, T.E., Briesmeister, J.F., Brown, F.B., Bull, J. S., Geisler, G.C., Goorley, J.T., Mosteller, R.D., 2004. MCNP^{TM} version 5. Nucl. Instrum. Methods Phys. Res. Sect. B Beam Interact. Mater. Atoms 213, 82–86.

Gaur, S., 1996. Determination of Cs-137 in environmental water by ion-exchange chromatography. J. Chromatogr. A 733. https://doi.org/10.1016/0021-9673(95)00906-X, 1–2.

Han, S.Y., Maeng, S., Lee, H.Y., Lee, S.H., 2020. Preliminary study on the detection efficiency and estimation of minimum detectable activity for a NaI(Tl)-based seawater monitoring system. J. Environ. Radioact. 218 https://doi.org/10.1016/j.jenvrad.2020.106222.

Knoll, Glenn F., 2010. In: Knoll, Glenn, F. (Eds.), Radiation Detection and Measurement, third ed. John Wiley & Sons.

Lee, J.-H., Byun, J.-I., Lee, D.-M., 2019. A two-point in situ method for simultaneous analysis of radioactivity in seawater and sediment. J. Radioanal. Nucl. Chem. 322 (2) https://doi.org/10.1007/s10967-019-06774-5.

Liang, D., Gong, P., Tang, X., Wang, P., Gao, L., Wang, Z., Zhang, R., 2019. Rapid nuclide identification algorithm based on convolutional neural network. Ann. Nucl. Energy 133, 483–490.

Osvath, I., Povinec, P.P., Livingston, H.D., Ryan, T.P., Mulsow, S., Commanducci, J.-F., 2005. Monitoring of radioactivity in NW Irish Sea water using a stationary underwater gamma-ray spectrometer with satellite data transmission. J. Radioanal. Nucl. Chem. 263 (2) https://doi.org/10.1007/s10967-005-0605-0.

Povinec, P.P., la Rosa, J.J., Lee, S.H., Mulsow, S., Osvath, I., Wyse, E., 2001. Recent developments in radiometric and mass spectrometry methods for marine radioactivity measurements. J. Radioanal. Nucl. Chem. 248 (3) https://doi.org/10.1023/A:1010696813200.

Soukissian, T.H., Chronis, G., 2000. Poseidon: a marine environmental monitoring, forecasting and information system for the Greek seas. Mediterr. Mar. Sci. 1 (1) https://doi.org/10.12681/mms.12.

Su, C.C., Su, C.-C., Huh, C.-A., Chen, J.-C., 2000. A Rapid Method for the Determination of 137 Cs in Seawater. A rapid method for the determination of Cs-37 in seawater, 11, 4. https://www.researchgate.net/publication/298847038.

Terada, H., Sakai, E., Katagiri, M., 1980. Environmental gamma-ray exposure rates measured by *in-situ* Ge(Li) spectrometer. J. Nucl. Sci. Technol. 17 (4) https://doi.org/10.1080/18811248.1980.9732580.

Tsabaris, C., Androulakaki, E.G., Ballas, D., Alexakis, S., Perivoliotis, L., Iona, A., 2021. Radioactivity monitoring at North Aegean sea integrating in-situ sensor in an ocean observing platform. J. Mar. Sci. Eng. 9 (1) https://doi.org/10.3390/jmse9010077.

Tsabaris, C., Bagatelas, C., Dakladas, Th, Papadopoulos, C.T., Vlastou, R., Chronis, G.T., 2008. An autonomous in situ detection system for radioactivity measurements in the marine environment. Appl. Radiat. Isot. 66 (10) https://doi.org/10.1016/j.apradiso.2008.02.064.

Tsabaris, C., Prospathopoulos, A., 2011. Automated quantitative analysis of in-situ NaI measured spectra in the marine environment using a wavelet-based smoothing technique. Appl. Radiat. Isot. 69 (10), 1546–1553.

Wang, P., Tang, X.-B., Gong, P., Huang, X., Wen, L.-S., Han, Z.-Y., He, J.-P., 2018. Design of a portable dose rate detector based on a double Geiger-Mueller counter. Nucl. Instrum. Methods Phys. Res. Sect. A Accel. Spectrom. Detect. Assoc. Equip. 879, 147–152.

Wang, Y., Zhang, Y., Wu, N., Wu, B., Liu, Y., Cao, X., Wang, Q., 2015. Monte Carlo simulation of in situ gamma-spectra recorded by NaI (Tl) detector in the marine environment. J. Ocean Univ. China 14 (3). https://doi.org/10.1007/s11802-015-2841-4.

Wedekind, Ch, Schilling, G., Grüttmüller, M., Becker, K., 1999. Gamma-radiation monitoring network at sea. Appl. Radiat. Isot. 50 (4) https://doi.org/10.1016/S0969-8043(98)00062-1.

Ye, M., Gong, P., Wu, S., Li, Y., Zhou, C., Zhu, X., Tang, X., 2021. Lightweight SiPM-based CeBr3 gamma-ray spectrometer for radiation-monitoring systems of small unmanned aerial vehicles. Appl. Radiat. Isot. 176, 109848.

Yudong, W., Xiaobing, L., Chi, Z., Rong, Z., Chaowen, Y., 2018. Comparison of two spectrum-dose conversion methods based on NaI(Tl) scintillation detectors. J. Instrum. 13 (6) https://doi.org/10.1088/1748-0221/13/06/T06004.

Zhang, Y., Wu, B., Liu, D., Lv, H., Feng, X., 2020. Research on minimum detectable activity (MDA) of underwater gamma spectrometer for radioactivity measurement in the marine environment. Appl. Radiat. Isot. 155 https://doi.org/10.1016/j.apradiso.2019.108917.